A Learning rule for Place Fields in a Cortical Model:Theta phase precession as a network effect

Silvia Scarpetta, Maria Marinaro
Dept. of Physics "E. R. Caianiello" University of Salerno, 84081 Baronissi (SA), IT
INFN, Sezione di Napoli, Gruppo Collegato di Salerno
INFM, Unità di Salerno; IIASS, Vietri sul Mare, (SA) IT

February 9, 2008

Abstract

We show that a model of the hippocampus introduced recently by Scarpetta, Zhaoping & Hertz ([2002] Neural Computation 14(10):2371-96), explains the theta phase precession phenomena. In our model, the theta phase precession comes out as a consequence of the associative-memory-like network dynamics, i.e. the network's ability to imprint and recall oscillatory patterns, coded both by phases and amplitudes of oscillation. The learning rule used to imprint the oscillatory states is a natural generalization of that used for static patterns in the Hopfield model, and is based on the spike time dependent synaptic plasticity (STDP), experimentally observed.

In agreement with experimental findings, the place cell's activity appears at consistently earlier phases of subsequent cycles of the ongoing theta rhythm during a pass through the place field, while the oscillation amplitude of the place cell's firing rate increases as the animal approaches the center of the place field and decreases as the animal leaves the center. The total phase precession of the place cell is lower than 360^o, in agreement with experiments. As the animal enters a receptive field the place cell's activity comes slightly less than 180^o after the phase of maximal pyramidal cell population activity, in agreement with the findings of Skaggs et al (1996). Our model predicts that the theta phase is much better correlated with location than with time spent in the receptive field. Finally, in agreement with the recent experimental findings of Zugaro et al (2005), our model predicts that theta phase precession persists after transient intra-hippocampal perturbation.

1 Introduction

In this paper we will show how the model of the hippocampus introduced in Scarpetta et al. (2002) is able to explain the theta phase precession phenomena: the observation that oscillation phases of the activities of hippocampal place cells systematically shift relative to the theta rhythm as the animal traverses the place fields (O'Keefe Recce 1993; Skaggs et al 1996).

The first part of the paper reviews the model, its learning rule, and the recall dynamics. Briefly, the model's learned states are encoded by both the amplitudes and the phases of the oscillating neural populations, enabling more efficient and robust information coding than in conventional models of associative memory. The learning rule to imprint such oscillatory states is a natural generalization of that used for static patterns in the Hopfield model, and is based on the STDP synaptic plasticity observed experimentally. In particular, long-term potentiation and depression of the synaptic efficacies depends on the relative timing of the pre- and post- synaptic activities during learning. A further step is introduced to allow imprinting of correlated patterns properly.

The second part of this paper shows how the model accounts for theta phase precession observed in rat hippocampus. During learning of each spatial location, our model imprints an oscillatory pattern of specific amplitude and phase relationship between neurons by modifying neural synaptic connection strengths. After learning, the network's response to external inputs reveals the encoded phase information, and thus phase precession, even though the external inputs do not have the phase information. The phase precession effect comes out from the crucial ability of our model to store both the amplitudes relationship and the phases relationship of the oscillatory patterns in the synaptic connections. Both the bell-shaped firing tuning curves (receptive fields) and the phase precession phenomena are a result of the network synaptic connections. In particular, the phase precession is an effect of the overlap between the imprinted place fields: if adjacent receptive fields do not overlap the firing tuning curve of each place cell is preserved but the phase precession does not occur.

The model agrees with the observation (Skaggs et al 1996) that the first spikes, as the animal enters the receptive field, come near the phase of the minimal pyramidal population average activity. The total phase precession of the place cells can be close to 360^o, but not larger than 360^o as found by O'Keefe Recce (1993) and Skaggs et al (1996). In our model, the theta phase of the place cell is a function of the animal location, almost insensitive to the animal' running speed (for speeds that do not exceed a critical value related to the network connections and pa-

rameters), and therefore the theta phase shows a better correlation with the animal location than with time, in agreement with the experimental results of O'Keefe Recce (1993) and Huxter et al. (2003).

Numerous computational models (Burgess et al 1994, Tsodyks et al 1996, Wallenstein et al 1997, Jensen and Lisman 1996, Bose et al 2000, Booth et al 2001, Yamaguchi 2003, and Lengyel et al 2003) have attempted to account for the mechanisms that underlie the phase precession observation, but a fully-satisfactory explanation is still lacking. Recently, to contrast the predictions of different models of phase precession, Zugaro et al (2005) have transiently turned off neuronal discharges for up to 250 ms and reset the phase of theta oscillations by stimulating the commissural pathway in rats. After recovery from silence, phase precession continued: the theta phase of the place cell immediately after the recovery was correlated with the new location of the animal, despite the transient silence and the theta phase reset. Our model is in agreement with these recent experimental findings.

2 The model

The model structure and elements are based on the physiological and anatomical findings in the CA3 hippocampal region. These regions contain the principle pyramidal cells and the inhibitory interneurons. The pyramidal cells project long range axons to other pyramidal cells and interneurons, whereas the interneurons project more locally. The model is based on the one introduced and analyzed by one of us with Li Zhaoping and John Hertz in a recent paper (Scarpetta et al 2002). We review here its main features, more details can be found in the paper above mentioned. The state variables, modeling the membrane potentials, are $\mathbf{u} = \{u_1, \ldots, u_n\}$ and $\mathbf{v} = \{v_1, \ldots, v_n\}$ respectively for the excitatory and inhibitory units. (We denote vectors by bold fonts.) The unit outputs, representing the probabilities of the cells firing (or instantaneous firing rates) are given by $g_u(u_1), \ldots, g_u(u_n)$ and $g_v(v_1), \ldots, g_v(v_n)$, where g_u andg_v are sigmoidal activation functions that model the neuronal input-output relations. The equations of motion are

$$\begin{aligned} \dot{u}_i &= -\alpha u_i - \beta_i^0 g_v(v_i) + \sum_j J_{ij}^0 g_u(u_j) + I_i, \\ \dot{v}_i &= -\alpha v_i + \gamma_i^0 g_u(u_i) + \sum_{j \neq i} W_{ij}^0 g_u(u_j). \end{aligned} \tag{1}$$

where α^{-1} is the membrane time constant (for simplicity assumed the same for excitatory and inhibitory units), J_{ij}^0 is the synaptic strength from excitatory unit j to excitatory unit i, W_{ij}^0 is the synaptic strength from excitatory unit j to inhibitory unit i, β_i^0 and γ_i^0 are the local inhibitory and excitatory connections within the E-I pair i, and $I_i(t)$ is the net input from other parts of the brain. The model units represent local populations of biological neurons that share common input, so the number of neurons represented by an excitatory unit may be different from the number of neurons represented by an inhibitory unit. In this minimal model we omit inhibitory connections between pairs, since the real anatomical long-range connections appear to come predominantly from excitatory cells. The sensory input $I_i(t)$ to the system, which drives the excitatory units, has a static part $\bar{I}_i$ and an oscillatory part $\delta I_i(t)$ modulated at the theta frequency. The static part $\bar{\mathbf{I}}$ of the input determines a fixed point $(\bar{\mathbf{u}}, \bar{\mathbf{v}})$, given by the solution of equations $\dot{\mathbf{u}} = 0, \dot{\mathbf{v}} = 0$ with $\mathbf{I} = \bar{\mathbf{I}}$.

Linearizing the equations (1) around the fixed point leads to

$$\begin{aligned} \dot{u}_i &= -\alpha u_i - \beta_i v_i + \sum_j J_{ij} u_j + \delta I_i \\ \dot{v}_i &= -\alpha v_i + \gamma_i u_i + \sum_j W_{ij} u_j \end{aligned} \tag{2}$$

where u_i and v_i are now deviations from the fixed point, $\delta\mathbf{I} \equiv \mathbf{I} - \bar{\mathbf{I}}$ is the oscillatory part of the sensory input, $\beta_i = g_v'(\bar{v}_i)\,\beta_i^0$, $\gamma_i = g_u'(\bar{u}_i)\,\gamma_i^0$, $W_{ij} = g_u'(\bar{u}_j)\,W_{ij}^0$, $J_{ij} = g_u'(\bar{u}_j)\,J_{ij}^0$. Henceforth, for simplicity, we assume $\beta_i = \beta$, $\gamma_i = \gamma$, independent of i.

Eliminating the v_i from (2), we have the second order differential equations

$$\ddot{\mathbf{u}} + (2\alpha - \mathsf{J})\dot{\mathbf{u}} + [\alpha^2 - \alpha\mathsf{J} + \beta(\gamma + \mathsf{W})]\mathbf{u} = (\partial_t + \alpha)\delta\mathbf{I}. \tag{3}$$

(We use sans serif to denote matrices) or, equivalently,

$$\left[(\partial_t + \alpha)^2 + \beta\gamma\right]\mathbf{u} = \mathsf{M}\mathbf{u} + (\partial_t + \alpha)\delta\mathbf{I} \tag{4}$$

$$\text{where} \qquad \mathsf{M} = (\partial_t + \alpha)\mathsf{J} - \beta\mathsf{W}\,, \tag{5}$$

The terms in the square bracket describe the local E-I pair dynamics, while M gives an effective coupling between the oscillating E-I pairs. Learning imprints patterns into M through the long range connections J and W. After learning, $\mathbf{u}$ depends on how $\mathbf{I}$ decomposes into the eigenvectors of M. Thus the network can selectively amplify or distort $\mathbf{I}$ in an imprinted-pattern-specific manner and thereby functions as input mapping into the subspace spanned by the imprinted patterns.

Following Scarpetta et al (2002), we distinguish a learning mode, in which the oscillatory patterns are imprinted while the connections J and W are ineffective, from a recall mode, in which connection strengths are effective and fixed. With appropriate learning kernel, the network during recall responds strongly (resonantly) to inputs similar to those learned or linear combinations of them, and weakly to other inputs not related to the imprinted patterns. The phases and the amplitudes of the oscillatory response will be a linear combination of the phases and the amplitudes, respectively, of the imprinted oscillations recalled by the input.

2.1 Learning oscillatory patterns

First, let's imprint a single oscillatory pattern, $\mathsf{P}^\mu(t) = \boldsymbol{\xi}^\mu e^{-\mathrm{i}\omega_0 t} + \text{c.c.}$ where c.c. denote complex conjugate, and $\boldsymbol{\xi}^\mu$ is a complex vector with components $\xi_j^\mu = |\xi_j^\mu| e^{i\phi_j^\mu}$. Following Scarpetta et al (2002), the synaptic strength

J_{ij} is shaped by the correlations of the activities, $u_j(t')$ and $u_i(t)$, in pre-synaptic and post-synaptic cells through

$$J_{ij} = \frac{1}{NT}\int_0^T \mathrm{d}t \int_{-\infty}^{\infty} \mathrm{d}t'\, u_i(t) A_J(t-t') u_j(t') \quad (6)$$

where $A_J(t-t')$ is the learning kernel that measures the strength of the synaptic change at time delays $\tau = t - t'$ between the pre-synaptic and post-synaptic activities. In the case when $A_J(t-t') = \delta(t-t')$ the learning rule becomes the conventional Hebbian learning with $J_{ij} \propto \int dt u_i(t) u_j(t)$ used in Li and Hertz (2000). To model the experimental results of STDP (Markram et al 1997, Bi & Poo 1998) the kernel $A(\tau)$ was taken as an asymmetric function of τ, mainly positive (LTP) for $\tau > 0$ and mainly negative (LTD) for $\tau < 0$. Analogously for the synaptic strength W_{ij} we write

$$W_{ij} = \frac{1}{NT}\int_0^T \mathrm{d}t \int_{-\infty}^{\infty} \mathrm{d}t'\, v_i(t) A_W(t-t') u_j(t'). \quad (7)$$

Since the connections J and W are ineffective during learning, the responses u_i and v_i are proportional to the imprinting input $P_i^\mu(t)$. Substituting them into eqs. (6) and (7) yields connections

$$\begin{aligned} J_{ij}^\mu &= \frac{2}{N}\mathrm{Re}\left[\tilde{A}_J(\omega_0)\, \xi_i^\mu \xi_j^{\mu *}\right] \\ W_{ij}^\mu &= \frac{2\gamma}{N}\mathrm{Re}\left[\frac{\tilde{A_W}(\omega_0)}{\alpha - \mathrm{i}\omega_0}\xi_i^\mu \xi_j^{\mu *}\right], \end{aligned} \quad (8)$$

where

$$\tilde{A}_{J,W}(\omega) = |\chi_0(\omega)|^2 \int_{-\infty}^{\infty} \mathrm{d}\tau\, A_{J,W}(\tau) \mathrm{e}^{-\mathrm{i}\omega\tau} \quad (9)$$

$$\text{with} \quad \chi_0(\omega) = \frac{\alpha - i\omega_0}{\alpha^2 + \beta\gamma - \omega_0^2 - 2\mathrm{i}\omega_0\alpha} \quad (10)$$

Note that $\mathrm{Im}\,\tilde{A}_{J,W}(\omega) = 0$ if $A_{J,W}(\tau)$ is symmetric in τ and that $\mathrm{Re}\,\tilde{A}_{J,W}(\omega) = 0$ if $A_{J,W}(\tau)$ is antisymmetric. The dependence of the neural connections J and W and the oscillator couplings M on $\xi_i^\mu \xi_j^{\mu *}$ is just a natural generalization of the Hebb-Hopfield factor $\xi_i^\mu \xi_j^\mu$ for (real) static patterns. This becomes particularly clear for kernels satisfying the following matching condition:

$$\tilde{A}_J(\omega_0) = \frac{\beta\gamma}{\alpha^2 + \omega_0^2}\tilde{A}_W(\omega_0), \qquad \text{at} \qquad \omega = \omega_0. \quad (11)$$

Then the oscillator coupling simplifies into a familiar outer-product form for complex vectors $\boldsymbol{\xi}$:

$$M_{ij}^\mu = -2\mathrm{i}\omega_0 \tilde{A}_J(\omega_0) \xi_i^\mu \xi_j^{\mu *}/N, \quad (12)$$

In the following we will always consider the case of matching kernels (11).

We are interested in generalizing eq. (8) and (12) to the case in which multiple correlated patterns have to be imprinted. To construct the corresponding matrices for multiple patterns, $\boldsymbol{\xi}^\mu$, $\mu = 1, .., N$, we use the rule proposed by Personnaz et al (1985) and Diederich and Opper (1997) (see also Hertz el al 1991) for learning static correlated patterns without errors in the Hopfield model. Thus we write, for N, linearly independent, correlated patterns $\boldsymbol{\xi}^\mu$,

$$J_{ij} = Re\left(\sum_{\mu\nu} \tilde{A}(\omega_0) \xi_i^\mu (Q^{-1})_{\mu\nu} \xi_j^{\nu *}\right) \quad (13)$$

where the $N \times N$ matrix Q, defined by

$$Q_{\mu\nu} = \frac{1}{N}\sum_j \xi_j{}^{\mu *} \xi_j{}^{\nu}, \quad (14)$$

is the natural generalization of the correlation matrix Q used by Personnaz et al (1985) and Diederich and Opper (1997) for the Hopfield model. The rule (13) is not local and not iterative. However it has been proved in Diederich and Opper (1997) that, in the Hopfield framework, there exists a local rule that uses only successive presentation of one pattern at a time that converges exactly to the synaptic efficiencies obtained with the Q-rule. Work is in progress to generalize their procedure, and obtain the same result also in our case. In the following, we have used the rule (13). With the rule (13), we imprint N oscillatory patterns $P^\mu = \xi^\mu e^{\mathrm{i}\omega_0 t}$, all with the same frequency ω_0. Then the M matrix becomes:

$$M_{ij} = \frac{1}{N}\sum_{\mu\nu} -2\mathrm{i}\omega \tilde{A}_J(\omega_0)\, \xi_i^\mu\, (Q^{-1})_{\mu\nu}\, \xi_j^{\nu *}, \quad (15)$$

2.2 The recall mode

In the recall mode the network dynamics is governed by the matrix M, learned during the learning mode. Keeping in mind eq. (15), it is clear that the imprinted oscillations (even though not-orthogonal) are eigenvectors of the connection matrix M,

$$\mathsf{M}\boldsymbol{\xi}^\gamma = -2\mathrm{i}\omega_0 \tilde{A}(\omega_0)\boldsymbol{\xi}^\gamma. \quad (16)$$

Thus, after the transient (which is governed by the network reaction time that depends both on the membrane time constant of the neurons, α, and the network synaptic connections), the response $\mathbf{u}$ to an input that perfectly match one of the imprinted vector is

$$\mathbf{u} = \chi \mathbf{I} \quad (17)$$

with the linear response coefficient (or susceptibility)

$$\chi = \frac{\alpha - i\omega_0}{\alpha^2 + \beta\gamma - \omega_0^2 - 2\mathrm{i}\omega_0\alpha + 2\mathrm{i}\omega_0\tilde{A}(\omega_0)} \quad (18)$$

A properly chosen learning kernel $A(t)$ satisfying

$$\begin{aligned} \alpha^2 + \beta\gamma - \omega_0^2 + 2\mathrm{i}\omega_0 \mathrm{Re}\left[\tilde{A}(\omega_0)\right] &\to 0 \\ \alpha - \mathrm{Im}\left[\tilde{A}(\omega_0)\right] &\to 0_+ \end{aligned} \quad (19)$$

would produce a very strong susceptibility χ and thus a resonant response to match input. Meanwhile, an input pattern $\mathbf{I}$ outside the subspace of the imprinted vectors evoke a weaker response $\mathbf{u} = \chi_0 \mathbf{I}$. In general, an input

$I = \boldsymbol{\xi} e^{i\omega t}$ that overlaps with several imprinted patterns will evoke a correspondingly mixed resonant response

$$\mathbf{u} = \chi \mathbf{I}_{\parallel} + \chi_0 \mathbf{I}_{\perp} \tag{20}$$

where $\mathbf{I} \equiv \mathbf{I}_{\parallel} + \mathbf{I}_{\perp}$, $\mathbf{I}_{\parallel} = \sum_\mu \langle \boldsymbol{\eta}^\mu | \boldsymbol{\xi} \rangle \boldsymbol{\xi}^\mu \mathrm{e}^{-\mathrm{i}\omega t} \equiv \sum_\mu N^{-1} (\sum_j \eta_j^{\mu *} \xi_j) \boldsymbol{\xi}^\mu \mathrm{e}^{-\mathrm{i}\omega t}$, and $\boldsymbol{\eta}^\mu = \sum_\nu Q_{\nu\mu} \boldsymbol{\xi}^\nu$.
This feature enables the system to interpolate between imprinted patterns, and to perform an elementary form of generalization from the learned set of patterns. As it will be shown in the next section, the phase precession as the animal moves from one location to the other is related to this interpolation mechanism.

An example of learning kernel $A(\tau)$ that satisfy the resonance conditions (19) at frequency $\omega_0 = 10$ Hz (theta range) is shown in Fig. 1. This learning kernel is able to imprint oscillations with frequency $\omega_0 = 10$ Hz, and to make the network resonant at theta frequencies. It could be of interest to note that the kernel $A(\tau)$ shown in Fig. 1 satisfies the resonance condition also at $\omega_0 = 40Hz$, i.e. in the gamma range. However we will not exploit this last property in this paper.

3 Imprinting locations and the theta phase precession

Let's consider N locations, x_μ arranged in a 1-dimensional space with periodic boundary conditions (such as in a circular or triangular track). For each of these N locations x_μ, $\mu = 1, .., N$ we imprint, in the synaptic strengths of the network, an oscillating pattern P^μ, with specific amplitude and phase relationship between its components. Using eq. (13) in order to imprint N (linearly independent) patterns, one need a number of network units $n > N$. In the following we use a network with n=2N excitatory units and the same number of inhibitory units, that follows the equation of motion (1). For each location x_μ an oscillating pattern P^μ, whose amplitude profile is peaked in the excitatory unit 2μ, is imprinted in the network. In particular, the imprinted pattern associated with location x_μ has components $P_j^\mu(t) = \xi_j^\mu \mathrm{e}^{-\mathrm{i}\omega_0 t} + \text{c.c.}$, $\mu = 1, 2, .., N$, $j = 1, 2, .., 2N$, where $\xi_j^\mu = \mathsf{A}(2\mu - j) e^{i\phi(2\mu - j)}$; the amplitudes A and the phases ϕ of the pattern $\boldsymbol{\xi}^i \mu$ on each unit j are functions of the distance between the unit j and the unit 2μ that is associated with location x_μ. In particular, $\mathsf{A}()$ is an even function decreasing quickly with distance, while $\phi()$ is an odd function. This means, when imprinting a location x_μ, only units located close to unit 2μ are excited by the imprinting inputs. In such a manner, after the learning process, the N excitatory units $u_{2\mu}$, that we will call place cells, will be associated with a receptive field centered at x_μ, for $\mu = 1, 2, \ldots, N$. The other N units (with odd index, called auxiliary units) are necessary in order to allow the network to store the N desired patterns properly. In all simulations we used $\mathsf{A}(0) = 1$, $\mathsf{A}(\pm 1) = 0.3$ $\mathsf{A}(\pm 2) = 0.3$, $\mathsf{A}(x) = 0$ otherwise, and $\phi(0) = 0$, $\phi(\pm 1) = \mp 2.4\, rad$ and $\phi(\pm 2) = \mp 2.5\, rad$. The network has a quite robust behavior with respect to the choice of the functions A and ϕ.

In our model the external inputs in the recall mode resembles but are not exactly the imprinted patterns. When the animal is exactly at location x_μ, the input pattern $\delta\mathbf{I}$ is given by $\delta\mathbf{I} = \mathsf{L}^\mu \mathrm{e}^{-\mathrm{i}\omega_0 t}$ where L^μ is a vector with components $L_j^\mu = \delta_{j,2\mu}$. This pattern conveys the animal location in the amplitude modulation but has no phase coded information. When the animal is at position x between location x_μ and location $x_{\mu+1}$, $x_\mu < x < x_{\mu+1}$, we take the input vector as linear combination of L^μ and $\mathsf{L}^{\mu+1}$,

$$\mathsf{L}^x = (1 - |x - x_\mu|)\mathsf{L}^\mu + |x - x_\mu| \mathsf{L}^{\mu+1} \tag{21}$$

L is then normalized. Thus, if the animal moves from location x_μ at time $t = 0$ to the adjacent one $x_{\mu+1}$ with speed $v(t)$, the current location will be a function of time $x(t) = x_\mu + \int_0^t v(t)dt$, and the input vector will be expressed by eq. (21) where x is replaced by $x(t)$. The vector L is always normalized. Fig. 2B shows the input amplitude $L_j(t)$ when animal moves along the track with constant speed.

A animal at location x receives an input pattern L^x that resembles imprinted pattern $\boldsymbol{\xi}^\mu$ for $x_\mu \approx x$. Hence, the network response to input L^x would amplify the imprinted pattern $\boldsymbol{\xi}^\mu$ that resembles L^x most (see previous section), and thus exhibits in the responses the non-trivial phase relationship among units that was stored in the couplings. When animal is in between two stored locations, the response will be a combination of the two imprinted patterns (see eq. (20)), and in particular, the phase of the response will be a combination of the phases of the two imprinted overlapping patterns which depends from the animal position. So, even though the input carries information about current location only in the amplitudes modulation, the associative memory nature of our model, having phase-coded locations imprinted in the synaptic couplings, allows the network to show both amplitude and phase coded informations in the response.

Since the theta rhythm is the local field potential, in our model it is simply the mean field. We compute the theta rhythm doing the average of all the excitatory units activities $M.F. = 1/2N \sum_{j=1}^{2N} u_j(t)$. This choice allows us to compare the the absolute phase of theta at which place cells fire during the place field traversal, with the experimental findings of Skaggs et al. (1996). Indeed, the phase zero of the theta rhythm in the experimental work of Skaggs et al 1996 is defined to be the point in the theta cycle corresponding to the maximal pyramidal cells population activity (i.e. the average over the entire dataset of pyramidal cells), and the EEG is opportunely shifted in order to agree with this definition of theta rhythm phase.

4 Simulation Results and comparisons with experimental findings

In all simulations reported here we used the kernel $A(t)$ shown in fig. 1 that satisfy the constraints (19) when $\omega_0 = 10Hz$, i.e. when the frequency is in the theta range.

After having imprinted $N = 10$ locations in the net with $n = 20$ excitatory units, we simulate the network

dynamics while the animal moves continuously in space. Fig. 2 shows in red the activity of the two place cell units ($u_{2\mu}$ with $\mu = 5, 6$), as a function of time, while the animal moves with constant running speed. Black curves shows the theta rhythm computed as the mean field of all the excitatory units of the network.

The simulation is done at a constant animal speed $v = 1/(400ms)$ (note that space is adimensional in our framework, and a unitary distance correspond to the distance between the centers of two adjacent receptive fields). The oscillatory input on each unit j is $I_j(t) = L_j(t)cos(\omega_0 t)$, where the amplitude $L_j(t)$ is shown in fig. 2B as a function of time. The figure shows that, for each place cell, the oscillation amplitude of the firing rate increases as the animal approaches the center of its place field and decrease as the animal left the center (firing tuning curve), while the place cell phase advanced at consistently earlier phases of the theta cycle as the animal pass through the cell's receptive field (phase precession). To quantify the phase precession phenomena, we compute the phase shift between the theta rhythm and the place cell activity in each cycle, and we plot in fig. 2 the theta phase as a function of the animal position during running, together with the amplitude modulation.

The model dynamics is in agreement with the experimental evidence of theta phase precession in two main points: 1) the total phase precession is less than 360^o (O'Keefe Recce 1993, Skaggs 1996); 2) as the animal enters the receptive field the absolute phase of the cell activity with respect to the phase of maximal excitatory units population activity (theta rhythm) is slightly less than 180^o, in agreement with experimental finding of Skaggs et al (1996).

Effects on nonlinearity in our general model have been analyzed in Scarpetta et al (2002), where we distinguished two class of nonlinearity. For the nonlinearity of class I (as the sigmoidal function shown in fig. 3B) we expect that the nonlinearity do not change critically the linear results. Indeed comparing the linear case in fig. 2 with the nonlinear simulations results shown fig. 3 we see that the dynamics is affected by the nonlinearity at large amplitudes but the phase precession is very well preserved.

To check if in our model the theta phase is better correlated with position than with time, we simulate the network dynamics with different values of the animal running speed. In fig. 4 the theta phase is shown as a function of animal position when animal runs with three different speeds ($v = 1/800ms^{-1}$ black squares, $v = 1/400ms^{-1}$ red triangles, and $v = 1/200ms^{-1}$ green circles). As we expect, the theta phase is a unique function of the animal position, almost insensitive to the running speed, as long as the reaction time of the network is short compared with the time characteristic of the animal movement. While, when the speed is large the inertia-like effects becomes significant and a (small) dependence from the speed appears (green circles follow a line with a higher slope) in the second half of the receptive field.

From figure 4 we see that, when there's variability in running speed, the phase shows a better correlation with position than with time. This is in agreement with experimental results os O'Keefe Recce (1993) and Huxter et al (2003).

Finally, in order to test our model, we compare it with the recent experiments of Zugaro et al 2005. We have simulated the effect of a perturbation that silences all units (both excitatory and inhibitory ones) and reset the phase of theta rhythm. The activity of two place cells, before during and after the network perturbation, is shown in fig. 5. The perturbation last for 200 ms. Despite the theta phase reset and the transient interruption of firing, the theta phase of the first cycle after the recovery is more advanced than the theta phase of the last cycle before the perturbation, as in the experiments (Zugaro et al 2005). The decrease of the peak firing rate is stronger in our simulations than in the experimental findings of Zugaro et al (2005), that reported only a small but not-significant decrease in peak firing rate. To quantify the degree of conservation of the phase precession and the effect on the amplitudes of oscillation we shows in fig. 5 the plot of the theta phase as a function of the position, and the amplitude of the oscillation versus the animal position. Figure 5C should be compared with fig. 2 in Zugaro et al (2005).

Figs. 6 and 7 show the synaptic connections J_{ik} and W_{ij} learned in our model, as a function of pre-synaptic cell index k, for a post-synaptic place cells (i even) and an auxiliary units (i odd). As expected, the synaptic connections are translation invariant, so J_{ij} depend only on the difference $i - j$ and on the parity of i (even or odd). We note that connections have both positive and negative values. Since they are supposed to be projections from excitatory pyramidal cells, the negative connections weights means effectively inhibitory connections, which could be implemented by additional inhibitory interneurons with very short membrane time constant. Note that the synaptic weights are highly asymmetric.

Finally, note that in our model the activity of all the units, both excitatory and inhibitory units, is modulated at the theta frequency. The network shows resonance in the theta range, and the inhibitory units, similarly to the place cells, exhibit phase precession (not shown), while the auxiliary units have a very weak place field with very little phase precession (not shown).

5 Conclusions and Discussion

In this paper we propose a theoretical model for theta phase precession in the hippocampus by applying a framework (Scarpetta Zhaoping Hertz 2002) that is a generalization of the Hopfield model to oscillatory patterns. The learning rule is a generalization of the Hebb prescription, inspired to the STDP synaptic plasticity.

The associative memory behaviour of our model, allows the network to show both amplitude and phase coded informations in response to inputs that carry information about current location only in the amplitudes modulation.

Our model dynamics is in agreement with the experi-

mental evidence of theta phase precession in 3 main points:

1) the model accounts for the observations that after a perturbation that transiently turned off neuronal discharges for a couple of theta cycles and reset the phase of the theta oscillations, the phase precession continued (Zugaro et al. 2005). This happens in our model, even if the external input to the network is silenced during the perturbation. This comes naturally from the fact that in our model, the oscillation phase of a place cell depends on both the network connections and the external input strength. Hence, when the external input strength represents the spatial location (relative to the center of the place field), the oscillation phase of the place cell will, by the influence of the network connections, code the location relative to the center of the place field.

2) In our model the theta phase depends on current position of the animal, and is only slightly sensitive to the animal speed (almost insensitive at low speeds). Therefore in our model the theta phase is better correlated with position than with time spent in the place field, in agreement with experimental data (O'Keefe Recce 1993, Huxter et al 2003). This is achieved without need of any speed-dependent input, in contrast with the recent model of phase precession (Lengyel et al 2003) that assumes a differential input proportional to the instantaneous velocity of the rat.

3) Both the initial theta phase as the animal enters the place field and the total phase precession generated by our network dynamics, are in quantitative agreement with experimental evidence. In our model the total phase precession is less than 360^o, and the absolute phase of the cell activity w.r.t. the average pyramidal cells activity, when the animal enters the place field, is slightly less than 180^o, in agreement with experiments of Skaggs et al. (1996). Note that our definition of the theta rhythm as the average activity of all the excitatory units is in agreement with the definition used by Skaggs et al (1996).

Finally note also that our model predicts both a monotonic phase precession and a unimodal firing tuning curve with a large amplification factor when the animal is in the center of the place field. This is in contrast with some other models. For example, models in which both firing rate and phase are linear or monotonic functions of the same parameter (Booth and Bose 2001; Magee 2001) produce a monotonically increasing firing rate inside the place field if monotonic phase precession is preserved, or non-monotonic phase precession if unimodality of the firing profile is to be preserved.

Although there is some controversy as to whether theta phase precession is linear (O'Keefe Recce 1993) or if theta phase is an accelerating function of position (Skaggs et al 1996, Yamagushi et al 2002), and if it's smooth or clusterized, its trend is undoubtedly monotonic (O'Keefe and Recce 1993; Skaggs et al 1996, Yamagushi 2002), since there is a systematic progressive phase retardation as the animal passes through the place field.

In contrast, experimental data indicates that firing rate changed in a non-monotonic waxing-waning manner (O'Keefe Recce 1993, Skaggs et al. 1996), even though there is some controversy as to whether phase precession accompanies skewed firing profiles (Mehta et al. 2002; Harris et al. 2002) or not (Huxter et al. 2003).

Our model shares some similarities to the one of Tsodyks et al 1996, since both are based on the associative memory properties of the network. In contrast with the Tsodyks et al (1996) work, here the couplings are computed using a mathematical learning rule and the network dynamics is studied analytically in a framework (Scarpetta et al 2002) that is the generalization of the Hopfield model to the case of not-static but oscillatory patterns.

A point of our model that still needs investigation is the origin of the imprinted patterns used during the learning mode. Of course, if there is no phase differences between units in the imprinted patterns, there would be no phase precession despite of learning and network dynamics. We are currently investigating how such phase differences arise in the imprinted patterns during learning, i.e. if they are generated by an initial asymmetry of the connections that produces the phase shift among units when the animal is moving, or if they are inherited from earlier stages input during learning. Anyway, what we have proven here is that when the network is equipped with such a synaptic connectivity the network dynamics shows phase precession and phase-coded response to sensory input that do not have any phase difference between units activities.

It has previously been suggested that phase coding occurs in the sensory input to the place cells (Burgess et al. 1994), and it has been shown that under that model individual place cells will show phase precession versus the average place cell activity (Burgess et al. 1993), as in our model. A difference with their model is that, even if we use a phase-coded activity during learning, once the network is equipped with the proper synaptic couplings, the phase precession occurs, when the animal run, without need of any phase coding in the sensory input.

Acknowledgements

The idea of this work originated from a discussion with L. Zhaoping. Authors would like to thank her for the useful discussions, comments, and the critical reading of the manuscript. We would like to thank also the anonymous referees for the useful criticisms and comments which allow us to improve the paper. This work was partially supported by INFN project FB11.

References

Bi GQ, Poo MM (1998) Synaptic modifications in cultured hippocampal neurons: dependence on spike timing, synaptic strength, and postsynaptic cell type. J. Neurosci. 18(24):10464-10472.

Booth V, Bose A (2001) Neural Mechanisms for generating rate and temporal coded in model CA3 pyramidal cells. J Neurophysiol. 85:2432-2445.

Burgess N, Recce M, O'Keefe J (1994) A Model of Hippocampal Function. Neural Network 7:1065-1081.

Burgess N, O'Keefe J, Recce M (1993) Using Hippocampal Place Cells for Navigation, Exploiting Phase Coding. Neural Information Processing Systems 5:929-936.

Diederich S, Opper M (1987) Learning of correlated patterns in spin-glass networks by local learning rules. Phys. Rev. Lett. 58(9):949-952.

Hertz J, Krogh A, Palmer RG (1991) Introduction to the Theory of Neural Computation, (Addison-Wesley, Redwood City CA).

Huxter J, Burgess N, O'Keefe J (2003) Independent rate and temporal coding in hippocampal pyramidal cells. Nature 425:828-831.

Jensen O, Lisman JE (1996) Hippocampal CA3 region predicts memory sequences: accounting for the phase precession of place cells. Learn Mem. 3(2-3):279-87.

Lengyel M, Szatmary Z, Erdi P (2003) Dynamically detuned oscillations account for the coupled rate and temporal code of place cell firing. Hippocampus 13(6):700-14.

Li Zhaoping, Hertz J (2000) Odour recognition and segmentation by a model olfactory bulb and cortex. Network 11(1):83-102

Magee JC (2001) Dentritic mechanism of phase precession in hippocampal CA1 pyramidal neurons. J.Neurophysiol. 86:528-532.

Markram H, Lubke J, Frotscher M, Sakmann B (1997) Regulation of synaptic efficacy by coincidence of postsynaptic APs and EPSPs. Science 275(5297):213-5.

Metha MR, Lee AK, Wilson MA (2002) Role of experience and oscillations in transforming a rate code into a temporal code. Nature 417:741-746.

O'Keefe J, Recce ML (1993) Phase relationship between hippocampal place units and the EEG theta rhythm. Hippocampus 3(3):317-330.

Personnaz L, Guy on I, Dreyfus G (1985) Information Storage and Retrieval in Spin Glass Like Neural Networks. J. Phys. (Paris) Lett. 46:L356.

Scarpetta S, Zhaoping L, Hertz J (2002) Hebbian imprinting and retrieval in oscillatory neural networks. Neural Computation 14(10):2371-96.

Tsodyks MV, Skaggs WE, Sejnowski TJ, McNaughton BL (1996) Population dynamics and theta rhythm phase precession of hippocampal place cell firing: a spiking neuron model. Hippocampus 6(3):271-80.

Wallenstein GV, Hasselmo ME (1997) GABAergic modulation of hippocampal population activity: sequence learning, place field development, and the phase precession effect. J. Neurophysiol. 78(1):393-408.

Yamaguchi Y, Aota Y, Mc Naughton B, Lipa P (2002) Bimodality of theta phase precession in hippocampal place cells in freely running rats. J. Neurophysiol. 87:2629-2642.

Yamaguchi Y (2003) A theory of hippocampal memory based on theta phase precession. Biol. Cybern. 89:1-9.

Zugaro MB, Mononcuit L, Buzsaki G (2005) Spike phase precession persists after transient intrahippocampal perturbation. Nature Neuroscience 9(1):67-71.

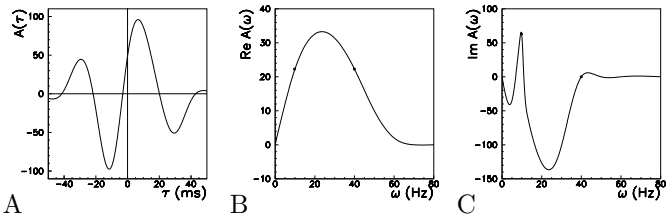

Figure 1: A. Example of a learning kernel $A(\tau)$ that satisfy the resonance conditions 18, at frequency $\omega_0 = 10Hz$. (Parameters $\gamma = \beta = 0.2ms^{-1}$, $\alpha = 0.14ms^{-1}$). The real (B) and the imaginary (C) part of its Fourier transform. In all the simulations we used the learning kernel shown in A.

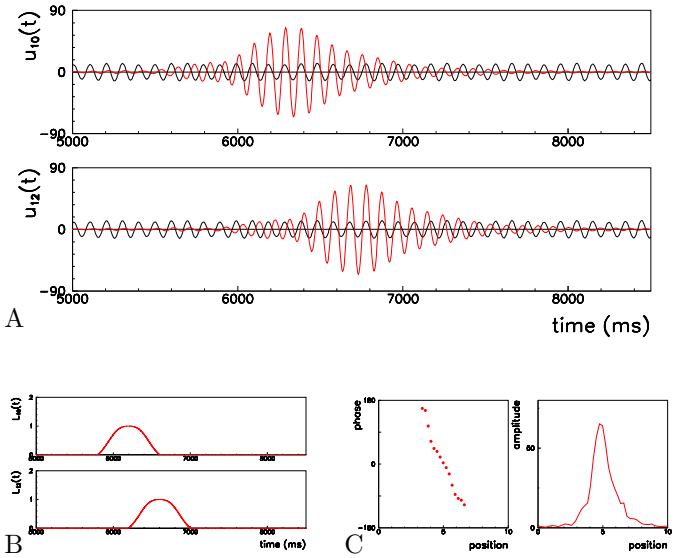

Figure 2: Simulation of the network dynamics when animal is moving continuously in time with constant running speed v=1/(200 ms). A: The two subplots show the activities (in dotted red) of two place cell units (u_j, $j = 10, 12$, whose place fields are centered at 5 and 6 respectively) as a function of time. Black curves show the ongoing theta rhythm activity (computed as the mean field of the excitatory activity of all the network). The external input to the units is $I_j(t) = L_j(t)cos(\omega_0 t)$, where the amplitude $L_j(t)$, shown in B, is maximum when the animal is in the center of the receptive field of that unit j. Note that each place cell unit shows phase precession, i.e., relative phase shift between $u(t)$ (red) and the theta activity (black), as the animal enters and then leaves the place field of this unit. Same behaviour for all other place cells not shown. C: Theta phase as a function of the current position of the animal, and amplitude of oscillation as a function of current animal position, for the place cell centered in location 5. Theta phase is a bit less than 180^o when the animal enters the receptive field, and the total phase precession is less than 360^o.

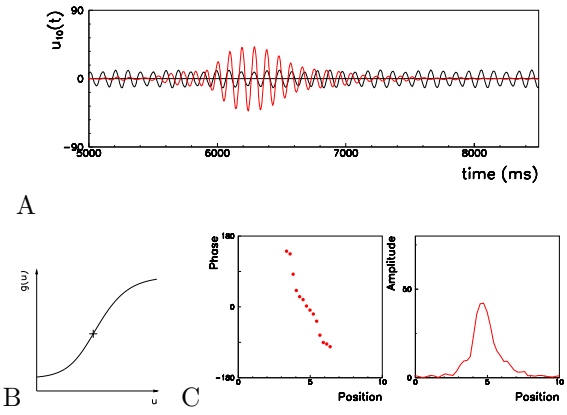

Figure 3: Effects of nonlinearity in the phase precession phenomena dynamics. A. Simulation of the network dynamics using the nonlinear activation function showed in B, when animal is moving continuously in time with constant velocity v=1/(200 ms) as in previous figure. Dotted red curve shows the place cell activity as a function of time. Black curves show the theta rhythm. Results are affected by nonlinearity mainly at large amplitude, but the theta phase precession is preserved, as shown in figure C showing the theta phase as a function of position, and amplitude of oscillation as a function of position for the place cell with receptive field centered in 5.

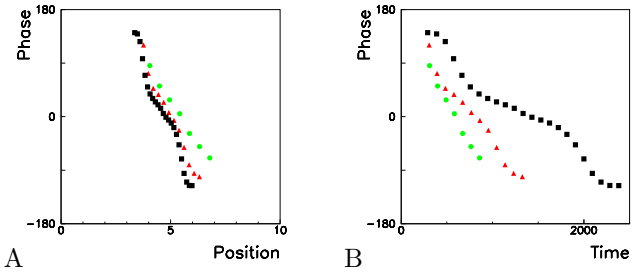

Figure 4: Theta phase of the place cell as a function of the animal position (A), and as a function of the time spent in the place field (B) at three different animal running speeds. During the place field traversal, for each cycle, we compute the phase of the place cell with respect to the theta rhythm. In each of the three simulations, the animal is moving continuously in time with constant speed. The green circles correspond to speed v=1/200 ms^{-1}, the red tringles to v=1/400 ms^{-1}, and the black squares to v=1/800 ms^{-1}. Figure shows that the theta phase is much better correlated with position than with time.

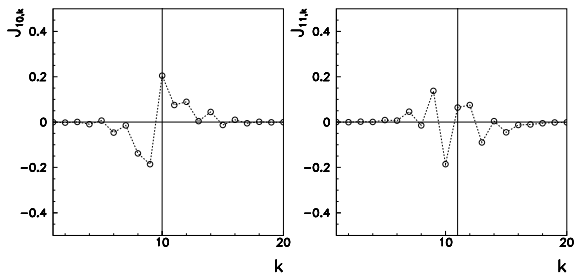

Figure 6: J_{ik} connection after learning N=10 locations, as a function of k. On the left, $i = 10$, and on the right, $i = 11$.

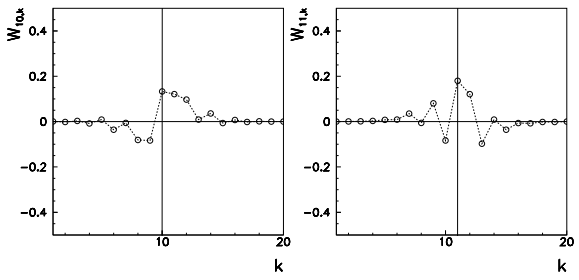

Figure 7: W_{ik} connection after learning N=10 locations, as a function of k. On the left, $i = 10$, and on the right, $i = 11$.

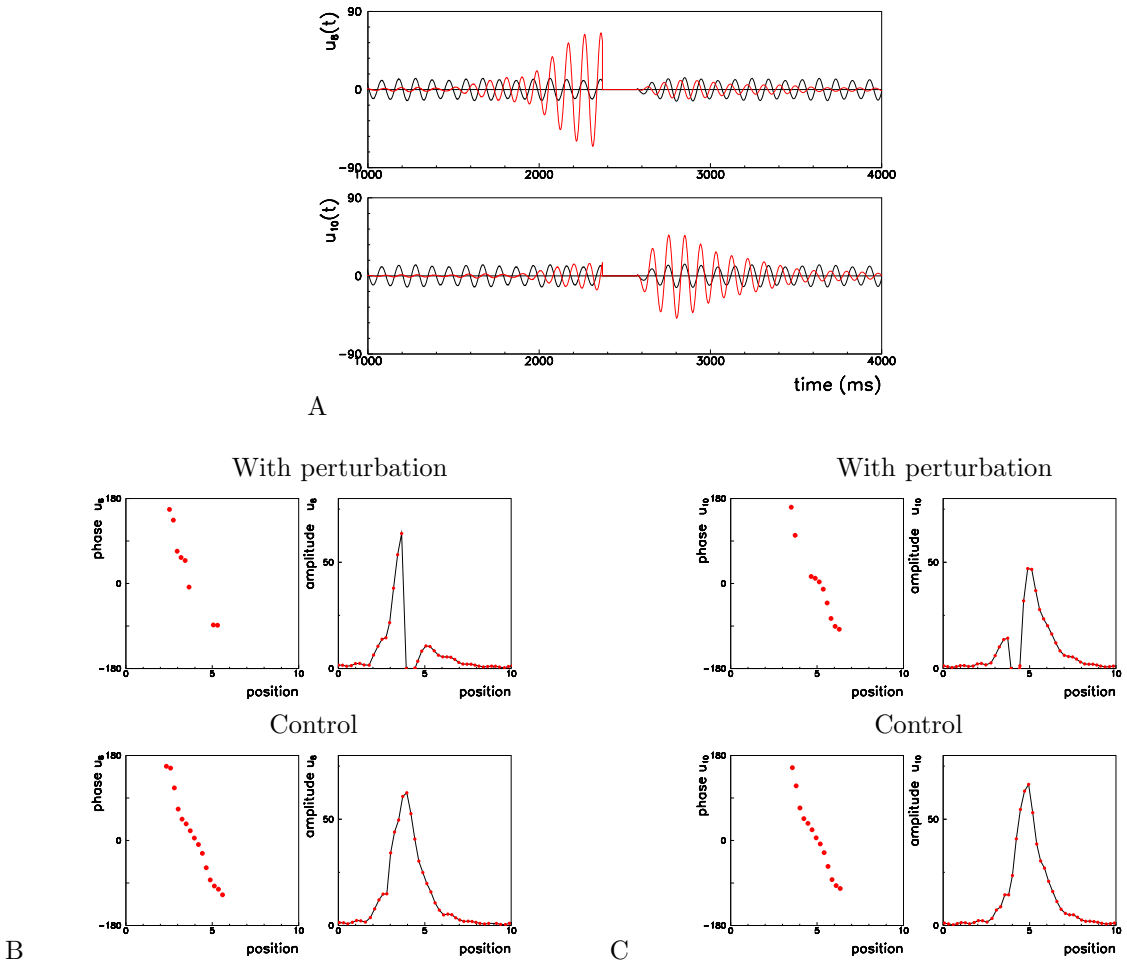

Figure 5: Phase precession persist after transient intra-hippocampal perturbation. Despite the theta phase reset and the transient interruption of firing, the phases were still correlated with the spatial position of the animal immediately after the recovery, in agreement with experiments (Zugaro et al 2005).A. Simulation of the network dynamics when animal is moving continuously in time with constant velocity v=1/(200 ms) but a perturbation that silences all units (both excitatory and inhibitory ones) and reset the phase of theta rhythm is applied for 200 ms. Black curves show the theta rhythm. The dotted red line shows the activity of the place cells before during and after the network perturbation (place cell u_8, centered in location 4, in the upper subplot, and place cell u_10, centered in 5, in the lower subplot). The theta phase and the firing amplitude are shown as a function of animal position when perturbation was applied, and in control conditions (i.e. without any perturbation), for the place cell centered in 4 (B) and the one centered in position 5 (C).